# Application of a Full 3-D Designature Solution to a Wide Azimuth Survey

*Jack Kinkead and Jon Burren PGS*

**Summary**

The current drive within the industry is towards a "Full Bandwidth" solution for seismic imaging coupled with acquisition solutions such as "Multi-Azimuth", "Wide-Azimuth" and "Full-Azimuth". Additionally, changes in source array geometry and multi-sensor receivers have also been employed. The proper processing of these types of data requires that special attention is given to how the wave field is produced, its propagation through the earth and finally how it is being captured. Of particular interest, and in order of their relative impact to the wave field, are:

- Surface ghost effects
- Source array effects
- Receiver array effects
- Earth effects

This paper will focus on the ghost and source array effects and the results achieved when they are handled properly.

**Introduction**

The dataset being used is from a survey acquired with a wide azimuth configuration in the predominantly deep water East Breaks area of the Gulf of Mexico circa 2009-2010 (figure 1).

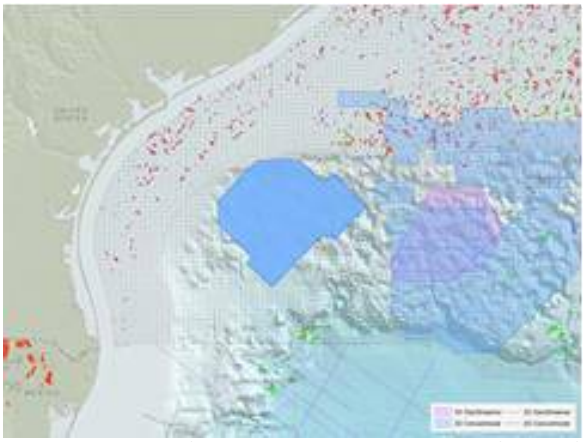

Figure 1: Location of survey in the East Breaks region of the Gulf of Mexico

A total of four vessels were deployed using two recording vessels with sources, each towing ten streamers; the diagram in figure 2 illustrates the acquisition geometry.

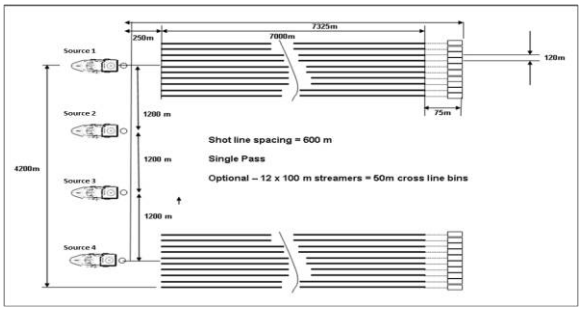


Figure 2: Diagram showing the geometry employed during acquisition of the wide azimuth survey

The fleet of vessels sailed back and forth in an interleaved pattern re-occupying source positions of the other vessels on alternate passes. By combining the records from similar shot positions a "super shot" is produced comprising a 70 streamer wide spread with the inner ten streamer positions duplicated (figure 3). The value of this style of acquisition over single vessel acquisition is well described in the literature e.g. Cambois *et al.* 2002, Long *et al.* 2006, Barley and Summers (2007).

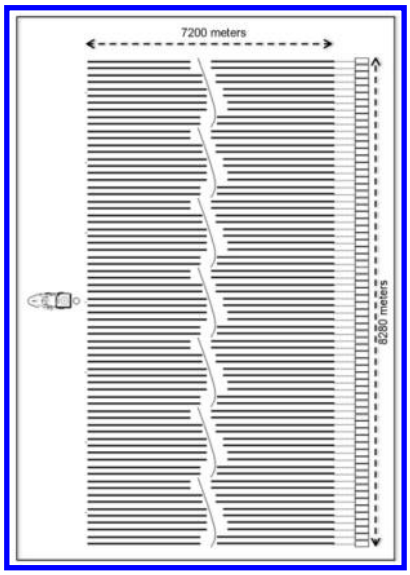


Figure 3: Diagram of super shot formed when combining sources from common locations

As mentioned previously, optimization of the spectral bandwidth requires several specific items be dealt with appropriately to obtain the broadest bandwidth and the correct phase response with this geometry.

The processes used to shape the effective wavelet on this dataset comprised the following stages which will be discussed in more detail individually.

- Removal of the source and receiver ghosts
- Initial shaping of the source signature using an average estimate of the source signature
- Residual correction filtering to compensate for the source array directivity

**Removal of the source and receiver ghosts**

Removal of the source side and receiver side ghosts was accomplished using a deterministic procedure, accounting for the 3D nature of the emission and emergence angles of the wave-field. The procedure utilizes depth information for the source and receiver to derive the appropriate amplitude and phase corrections.

The result of removing the ghost effects is illustrated in figure 4, showing a zoom over the flattened water bottom horizon. Moving left to right through the image, a simpler and sharper water bottom reflector is observed as each ghost effect is removed, implying improved resolution.

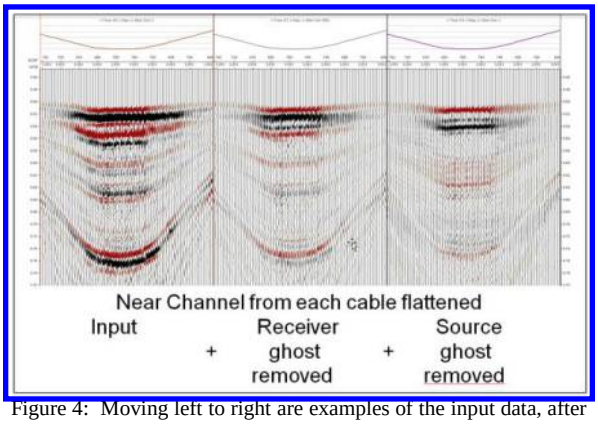


Figure 4: Moving left to right are examples of the input data, after removal of the receiver ghost only and after removal of both receiver and source ghosts

**Source de-signature using an extracted source estimate**

With the ghosts removed, the full effect of the bubble can be clearly observed in both the data and the survey-averaged extracted signature. Using this average signature, a filter was designed to compress the wavelet to a zero phase wavelet with a desired spectral response. In the signature extraction process only data from the near offsets were used in order to estimate the average vertical response of the source. In figure 5, the extracted signature is displayed along with the filtered result. Note the dominant bubble energy present and how well the shaping filter produces the desired wavelet response.

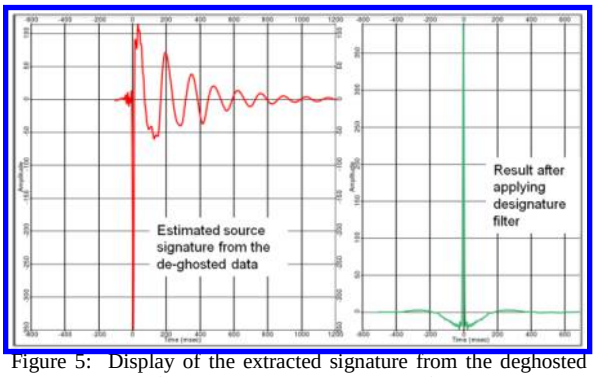


Figure 5: Display of the extracted signature from the deghosted data on the left and the ouput wavelet after applying the designature filter.

**3D source directivity corrections**

Analysis of the data volume after application of the de-signature filter indicated the need for additional shaping of the source wavelet. This is most prevalent at larger emission angles and crossline azimuths. While the water bottom reflection event appears as a well behaved wavelet at near emission angles, for larger angles and large crossline azimuths the wavelet exhibits an undesired change in shape (figure 6).

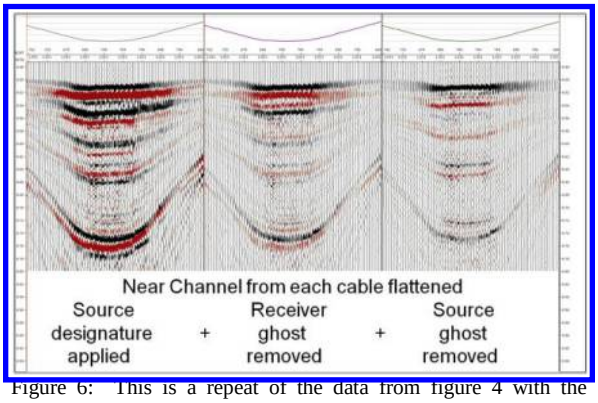


Figure 6: This is a repeat of the data from figure 4 with the application of the designature filter. Note how the center portion of each display exhibits a well behaved wavelet shape, as you move outward the events take on a lower frequency stretched appearance.

To better understand this behavior, it is necessary to consider the source geometry in more detail. Methods for modelling and analyzing the behavior of source arrays and their constituting components can be found in the literature – e.g. Ziolkowski *et al.* (1982), Parkes *et al*. (1984) and Mingqiang *et al*. (2014) – and some have been incorporated into powerful, commercially available software packages.

The source array for this survey comprised five sub-arrays laid out in parallel. The physical dimensions of the full source array are shown in figure 7 (top); the array forms a rectangular box 32 meters wide and 14 meters long. Figure 7 (bottom) also shows the modeled source wavelet for a constant emission angle of 60 degrees and azimuths encompassing the full 360 degrees. These directional variations in behavior indicate a possible explanation for the earlier observation.

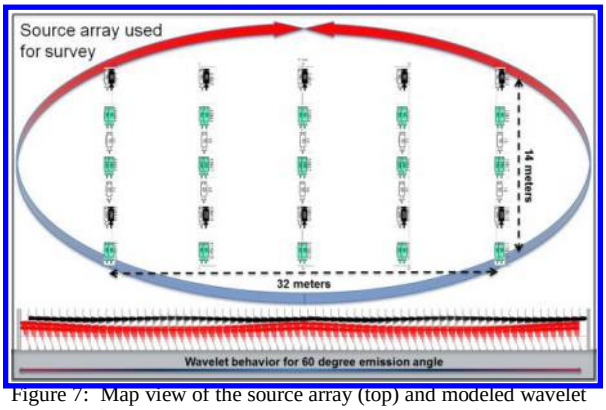


Figure 7: Map view of the source array (top) and modeled wavelet response for a 60 degree emission angle and the full range of azimuths (bottom).

Additional source modeling was performed targeting the same emission angles and azimuths for water bottom reflections in the data and the results compared with the real data (figure 8); the observed behavior was found to be clearly consistent with the modeled source response.

With the explanation validated, the next step was to compute differential correction filters corresponding to the azimuth and emergence angles at the source. These filters were applied to the data providing consistent behavior of the reflection events for all angles and azimuths (figure 9).

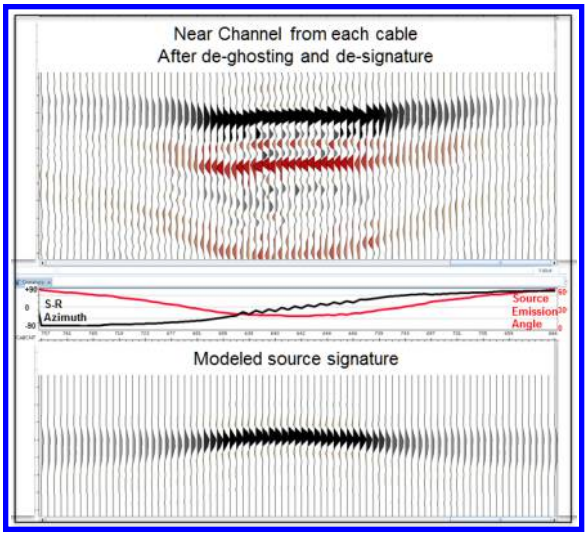


Figure 8: Fully deghosted data after designature (top) and the equivalent modeled response (bottom) for same range of emission angles and azimuths. There is a good correlation between the behaviour of the wavelet observed in the data and the modeled response.

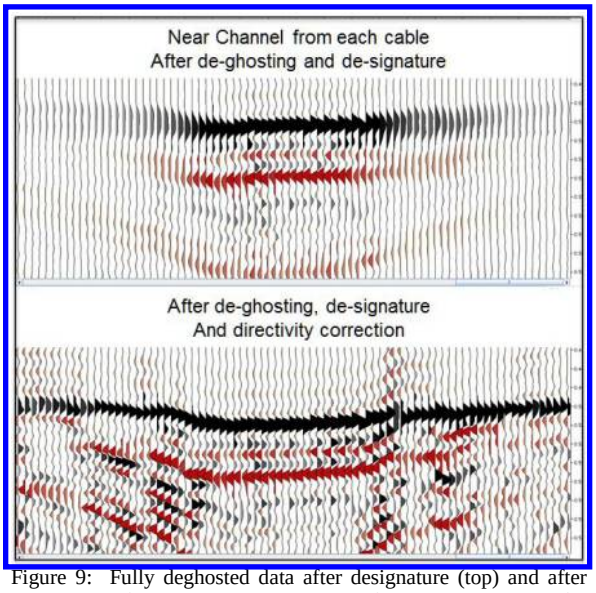


Figure 9: Fully deghosted data after designature (top) and after application of residual source correction filters to compensate for the directivity of the source array (bottom). Note how the reflection event at the water bottom is more stable.

## Conclusions

Deep water, wide azimuth datasets can provide sufficient sampling of the wave field allowing directional variations in the wavelet to be observed. The application of 3D de-ghosting for both the source and receiver side effects takes significant steps in optimizing the bandwidth whilst also correcting for some of the directionality. The traditional source signature deconvolution (designature) incorporating directional (3D) characteristics of the source array – observed in the data and validated though modeling – must also be addressed in order to fully optimize the available bandwidth of the recorded data.

The subsequent improved wavelet response will have a notable impact on the resolution of the reflection events in the shallow data; combined with improved consistency at the larger angles and large crossline azimuths, this will improve velocity analysis though the shallow section yielding improvements for deeper imaging. This can only be achieved through the proper handling of the source wavelet response, ghost effects, receiver array effects, and instrumentation filters (the earth effects must also be considered but have not been discussed here).

Advances in technology such as multi-component streamers (e.g. Tabti *et al*. 2009), more complex source designs and firing schemes, do not necessarily discount the need for what has been described here (and may further complicate how such corrections are made!). They should allow for more robust and accurate corrections to be made yielding higher quality results.

## Acknowledgments

The authors wish to thank PGS for permission to publish this work. Also a special thanks to our coworkers for their invaluable assistance and support

**EDITED REFERENCES**

Note: This reference list is a copyedited version of the reference list submitted by the author. Reference lists for the 2017 SEG Technical Program Expanded Abstracts have been copyedited so that references provided with the online metadata for each paper will achieve a high degree of linking to cited sources that appear on the Web.

**REFERENCES**

Brian, B., and T. Summers, 2007, Multi-azimuth and wide-azimuth seismic: Shallow to deep water, exploration to production: The Leading Edge, **26**, 450–458, https://doi.org/10.1190/1.2723209.

Cambois, G., S. Ronen, and X. Zhu, 2002, Wide-azimuth acquisition: The Leading Edge, **21**, 763.

Long, A. S., E. Fromyr, C. Page, W. Pramik, and R. Laurain, 2006, Multi-Azimuth and Wide-Azimuth lessons for better seismic imaging in complex settings: ASEG Extended Abstracts, 1–5, https://doi.org/10.1071/ASEG2006ab098.

Mingqiang, C., N. Chengzhou, L. Baojun, T. Liqing, and C. Lin, 2014, A Method of the Air gun Array Directivity Analysis: Beijing 2014 International Geophysical Conference and Exposition, 33–36, https://doi.org/10.1190/IGCBeijing2014-009.

Parkes, G. E., L. Hatton, and T. Haugland, 1984, Marine source array directivity: A new wide airgun array system: First Break, **2**, 9–15, https://doi.org/10.3997/1365-2397.1984013.

Tabti, H., A. Day, T. Schade, M. Lesnes, and T. Høy, 2009, Conventional versus dual-sensor streamer data de-ghosting: A case study from a Haltenbanken survey: First Break, **27**.

Ziolkowski, A., G. Parkes, L. Hatton, and T. Haugland, 1983, The signature of an air gun array: Computation from near-field measurements including interactions: Geophysics, **47**, 1413–1421, https://doi.org/10.1190/1.1441289.